How to efficiently apply soft thin coating to existing Finite Element contact model

Tauno Tiraats, Nicolas Chevaugeon, Nicolas Moës, Claude Stolz, Nabil Marouf, E Desdoit

How to efficiently apply soft thin coating to existing Finite Element contact model

T.Tiirats[a,b,*], N.Chevaugeon[a], N.Moës[a], C.Stolz[a,c], N.Marouf[b], E.Desdoit[b]

[a] *École Centrale de Nantes, Institut GeM UMR CNRS 6183, 1 Rue de la Noë, Nantes, France*
[b] *Vallourec Research Center France, 60 Rue de Leval, Aulnoye-Aymeries, France*
[c] *IMSIA UMR CNRS 9219, 91762 Palaiseau Cedex, France*

Abstract

In case of very thin surface coatings, the coating layer is often ignored in a large-scale Finite Element Analysis. This is mainly due to extensive numerical cost required to capture the correct mechanical behaviour of the layer, especially if the coating is significantly softer than the substrate.
To overcome the excessive computational cost, due to the full discretization of the thin layer, in large-scale structural contact simulations one can consider a polynomial approximation of the solution field inside the layer. This formulation allows for a reduced representation of the surface layer and proves to be suitable for incorporation within existing finite element codes. Inclusion of the method scales down to an additional stiffness to the system of equations. Furthermore, it can be used in a classical finite element contact solver without strong additional modifications.
Significant computational cost reduction is obtained for proposed 2D test-cases in comparison to fully discretized layer approach. It is especially apparent with soft layers on harder substrates. Hence, it is a promising method to be used in large scale structural simulations for studying the mechanical behaviour of systems with thin soft coatings.

Keywords: Thin coating, Polynomial expansion, Contact,

1. Introduction

In the case of thin coatings on large structures, the mechanical contribution of the layer in macro-scale finite element analysis is often ignored or modelled using structural elements like shells or membranes. However, due to the imposed kinematics in structural finite elements they are mainly suitable for stiff coatings. When focusing on soft coatings, with significant deformation along the thickness, different method needs to be used.

Traditional finite elements with high aspect ratio or with reduced dimension worsen the conditioning of the system of equations, possibly leading to an ill-conditioned system.

*Corresponding author
Email addresses: tauno.tiirats@ec-nantes.fr (T.Tiirats), nicolas.chevaugeon@ec-nantes.fr (N.Chevaugeon), nicolas.moes@ec-nantes.fr (N.Moës), claude.stolz@ec-nantes.fr (C.Stolz), nabil.marouf@vallourec.com (N.Marouf), emmanuel.desdoit@vallourec.com (E.Desdoit)

Therefore, performing a large scale analysis with soft thin coatings is often avoided due to extensive numerical cost involved to capture the correct behaviour of the layer. However, not always can the coating be discarded or modelled with standard finite elements, especially in nonlinear problems like contact. A good example of this is the Oil County Tubular Goods (OCTG) industry, where grease based lubrication of tubular connections in oil wells and transport lines are being replaced by polymer based coating systems. It is crucial for the evaluation of the tightening torque to have an accurate description of the contact pressures formed in the coated connection parts. This includes "metal-to-metal" seals where the effect of nearly incompressible coating material is significant on the stress distribution.

First the general context is defined. One considers a contact problem with significant geometrical and material scale differences: the coating thickness to contact half-width ratio is taken as $e/a \ll 1$ and the ratio of elastic Young moduli as $E_c/E_s \ll 1$, where c notes the coating and s the substrate materials. Therefore, under the contact zone significant amount of deformation is taking place inside the layer. This induces a strong influence on the contact pressure distribution.

As layer thickness reduces, the behaviour closes to a limiting case. Thus asymptotic modelling principles are often used to tackle this type of problems. The first asymptotic solutions for thin layer coatings were presented by Aleksandrov [1], Meijers [2] and Alblas & Kuipers [3]. Meijers and Alblas introduced also stable solutions for incompressible elastic materials. Using Hertzian theory Johnson formulated in [4] the limiting asymptotes corresponding to the previous works. A concise analysis of mentioned works and an addition of a more general semi-analytical solution is presented by Greenwood & Barber [5]. The change from linear elasticity to viscoelasticity and the dependency with respect to the thickness of the layer are studied in many other works by Argatov and Mishuris in [6, 7, 8]. A full depth semi-analytical analysis involving deformable substrates and rough surface contact models is presented by Goryacheva in [9].

For more complex geometries and material systems discretization based methods like FEM should be introduced. In general practice with FEM, thin solid structures are often modelled as shells or membranes. These structural elements are well suitable for simulation of problems with hard coatings $E_c/E_s > 1$. However, considering considerably softer coatings than the substrate, the usage of shells or membranes is questionable. This originates from the fact that the deformation gradient due to contact pressure in the coating layer itself can not be neglected or considered uniform in the thickness, especially in the case of nearly incompressible materials. This includes alternatives like solid-shell (continuum-shell) type of elements or Cosserat type shell elements [10] that allow for limited deformation through the thickness.

This leads to inclusion of non-standard models, like the imperfect interface model for very thin interfaces in composite materials by Hashin [11] and Benveniste & Miloh [12]. They replaced the thin layer by an interphase on what imperfect interface conditions are derived. The derivation by Benveniste [12, 13] is based on an asymptotic expansion in the interphase. Givoli further expanded the idea for usage in FEM [14] by the means of Dirichlet-to-Neumann interphase boundary conditions. In this case the boundary conditions become the interface jump conditions. Sussman in [15] renders the proposed model self-adjoint to result in a symmetric FE stiffness matrix, Yvonnet in [16] implemented it in XFEM framework and Rubin & Benveniste in [17] introduced Cosserat shell theory for stiff interphases, allowing limited thickness directional deformation.

Another interesting idea of modelling thin interfaces based on asymptotic considerations can be taken from the third-body wear models. In the works of Dragon-Louiset [18] an asymptotic expansion is used to define the behaviour of the thin interface of the "third body" that can be solved by FEM or analytically by the integral equations. In [19, 20, 21] Stolz proposes to introduce the behaviour of the layer as an interface with mechanical properties defined by a process of averaging over the thickness. For some particular classes of local behaviour described by an asymptotic expansion with respect to coordinate along the thickness, interface models are obtained. This is used to model contact and wear processes.

In this work, a numerical model is developed for soft coatings (low shear stiffness) that could be considered on large-scale models and included in contact and wear simulations. The main goal is to be compatible with FEM and provide a good approximation of the physics while introducing minimal additional computational effort. It follows the previously presented ideas of reducing the layer into an interface and considering an expansion based solution field approximation. Matthewson [22] presented a simplified analytical analysis of frictionless contact of a sphere and a thin elastic layer bonded to the rigid surface using finite power series. Even though his work considers specific layer indentation problem, one can see the potential in using polynomial based approximation together with FEM to provide a more general numerical framework. Therefore, given work tries to develop a more general polynomial expansion based numerical model for coating contact simulations.

In this paper the formulation of the model for a simple plain strain coating substrate system is presented. A rigid indentation problem is considered on a coating with uniform thickness on flat surface. An example of the implementation in the two-body contact framework is presented. The paper is structured as follows: section 2 involves description of the developed methodology including problem statement and implementation in FE framework; section 3 includes the description of the model implementations and the corresponding results; section 4 includes the discussion on the computational aspects; section 5 includes the main conclusions and outlooks.

2. Methodology

2.1. Problem statement

The domain of interest is a thin film Ω_e with uniform thickness e laying on an initially flat semi-infinite deformable foundation Ω. The interface between the two domains is defined by surface Γ_0, where $y = 0$. As plain strain formulation is used to simplify the method description, only the cross-section in xy-plane is considered, thus the displacement vector is introduced as $\boldsymbol{u}_a = u_a(x, y)\boldsymbol{e}_x + v_a(x, y)\boldsymbol{e}_y$. A pressure distribution $\boldsymbol{t}(x)$ corresponding to an arbitrary rigid indenter shape is applied on the area of $2a$ on the top surface Γ_e. The geometry of the area of interest is illustrated in figure 1.

The displacement field in the coating layer can be defined by a polynomial expansion with terms P_i in the layer thickness direction y and the unknown displacement coefficient

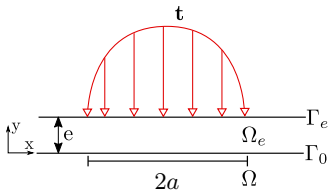

Figure 1: Illustration of the initial semi-infinite problem around the area of interest.

fields $\boldsymbol{u}_i$. In this case the displacement is decomposed as

$$\boldsymbol{u}_a(x,y) = \begin{cases} \boldsymbol{u}(x,y), & \text{in } \Omega \\ \boldsymbol{u}_0(x) + \sum_{i=1}^{n} P_i(y)\boldsymbol{u}_i(x), & \text{in } \Omega_e \end{cases} \tag{1}$$

with the continuity condition

$$\boldsymbol{u}_0(x) = \boldsymbol{u}(x,0) \quad \text{on } \Gamma_0, \tag{2}$$

with $P_i(0) = 0$. The domain Ω_e defines the layer with thickness e, thus y varies from 0 to e (or $e(x)$ in case of non-uniform thickness). The material interface is defined as $\Gamma_0 = \partial\Omega \cap \partial\Omega_e$ where $y = 0$ and the top surface defined as $\Gamma_e = \partial\Omega_e/\Gamma_0$ where $y = e$.

For example if one follows the idea of Matthewson [22] and uses a finite power series, the expansion will take the following form

$$\sum_{i=1}^{n} P_i(y)\boldsymbol{u}_i(x) = \sum_{i=1}^{n} \frac{y^i}{i!}\boldsymbol{u}_i(x) \ . \tag{3}$$

However, it is emphasized that any polynomial basis could be used instead.

Inside the domain, the conservation of momentum is expressed as

$$\nabla \cdot \boldsymbol{\sigma} = \mathbf{0} \ , \tag{4}$$

where the body forces are neglected and $\boldsymbol{\sigma}$ is the Cauchy stress. The continuity condition on the interface Γ_0 is satisfied by $[\boldsymbol{\sigma}] \cdot \boldsymbol{n} = \mathbf{0}$. As the domain is considered semi-infinite the external boundaries, excluding Γ_e, are considered to be significantly far from the area of interest. Thus, it is considered that $\boldsymbol{u}_a = \mathbf{0}$ on all boundaries where no coating exists. On the top surface Γ_e traction $\boldsymbol{t}$ is prescribed as

$$\boldsymbol{\sigma} \cdot \boldsymbol{n} = \boldsymbol{t}, \quad \text{over } \Gamma_e^t = \{x \in [-a,a], y = e\} \quad \text{and} \quad \boldsymbol{\sigma} \cdot \boldsymbol{n} = \mathbf{0} \text{ otherwise.} \tag{5}$$

Finally the local behaviour inside the layer is considered linear elastic by stating

$$\boldsymbol{\sigma} = \mathbb{C} : \boldsymbol{\epsilon}, \qquad \boldsymbol{\epsilon} = \nabla^s \boldsymbol{u}_a = \frac{1}{2}(\nabla \boldsymbol{u}_a + \nabla^T \boldsymbol{u}_a), \tag{6}$$

where $\mathbb{C}$ accounts for the constitutive tensor for isotropic elasticity with $\mathbb{C}(E_s, \nu_s)$ in Ω and $\mathbb{C}(E_c, \nu_c)$ in Ω_e. The symbols E_c and ν_c refer to the Young modulus and the Poisson's ratio of the coating material and E_s with ν_s of the substrate material. Here it is considered that the surface coating material is significantly softer than the foundation, particularly $E_c/E_s < 10^{-3}$.

105 *2.2. Problem analysis*

For derivation purposes, the considered expansion will be the finite power series defined in equation 3. The displacement in the thin layer is now decomposed into foundation term $\boldsymbol{u}_0(x)$ and film term $\boldsymbol{u}_e(x,y)$ as

$$\boldsymbol{u}_0(x) = u_0(x)\boldsymbol{e}_x + v_0(x)\boldsymbol{e}_y \ , \tag{7}$$

$$\boldsymbol{u}_e(x,y) = \sum_{i=1}^{n} \frac{y^i}{i!} u_i(x)\boldsymbol{e}_x + \sum_{i=1}^{n} \frac{y^i}{i!} v_i(x)\boldsymbol{e}_y \ . \tag{8}$$

Furthermore, the solution space is noted as $\mathcal{U}$ and the test space as $\mathcal{U}_0$.

The weighted weakform is obtained by dotting equation 4 with an arbitrary $\boldsymbol{u}_a^* \in \mathcal{U}_0$ and integrating over the domain $\Omega_e \cup \Omega$. The resulting equation to solve reads

$$\begin{aligned} &\int_\Omega \boldsymbol{\sigma}(\boldsymbol{u}) : \boldsymbol{\epsilon}(\boldsymbol{u}^*)\ \mathrm{d}\Omega + \int_{\Omega_e} \boldsymbol{\sigma}(\boldsymbol{u}_a) : \boldsymbol{\epsilon}(\boldsymbol{u}_0^*)\ \mathrm{d}\Omega + \int_{\Omega_e} \boldsymbol{\sigma}(\boldsymbol{u}_a) : \boldsymbol{\epsilon}(\boldsymbol{u}_e^*)\ \mathrm{d}\Omega \\ &- \int_{\Gamma_e} \boldsymbol{t}\cdot\boldsymbol{u}_0^*\ \mathrm{d}\Gamma - \int_{\Gamma_e} \boldsymbol{t}\cdot\boldsymbol{u}_e^*\ \mathrm{d}\Gamma = 0, \qquad \forall \boldsymbol{u}^*, \boldsymbol{u}_0^*, \boldsymbol{u}_e^* \in \mathcal{U}_0 \end{aligned} \tag{9}$$

To better illustrate all the components let us emphasize the dependencies as $\boldsymbol{u}_e = \boldsymbol{u}_e(u_i, v_i)$ and write the solution in variational equations form as

$$\boldsymbol{u}^* \rightarrow \quad \int_\Omega \boldsymbol{\sigma}(\boldsymbol{u}) : \boldsymbol{\epsilon}(\boldsymbol{u}^*)\ \mathrm{d}\Omega + \int_{\Omega_e} \boldsymbol{\sigma}(\boldsymbol{u}_0 + \boldsymbol{u}_e(u_i,v_i)) : \boldsymbol{\epsilon}(\boldsymbol{u}_0^*)\ \mathrm{d}\Omega = \int_{\Gamma_e} \boldsymbol{t}\cdot\boldsymbol{u}_0^*\ \mathrm{d}\Gamma \tag{10}$$

$$\boldsymbol{u}_e^* \rightarrow \quad \int_{\Omega_e} \boldsymbol{\sigma}(\boldsymbol{u}_0 + \boldsymbol{u}_e(u_i,v_i)) : \boldsymbol{\epsilon}(\boldsymbol{u}_e^*(u_i,v_i))\ \mathrm{d}\Omega = \int_{\Gamma_e} \boldsymbol{t}\cdot\boldsymbol{u}_e^*(u_i,v_i)\ \mathrm{d}\Gamma \ . \tag{11}$$

It is interesting to note that in this case the strain tensor in the layer takes the following form (zero row/column discarded) and can be decomposed into multiple separate tensors, each corresponding to a given power series term.

$$\boldsymbol{\epsilon}_{|\Omega_e} = \boldsymbol{\epsilon}_0 + \sum_{i=1}^{n} \frac{y^i}{i!}\boldsymbol{\epsilon}_i = \sum_{i=0}^{n} y^i c_i \boldsymbol{\epsilon}_i \ , \qquad \text{where } c_i = (i!)^{-1} \tag{12}$$

and

$$\boldsymbol{\epsilon}_0 = \begin{bmatrix} u_{0,x} & \frac{1}{2}(u_1 + v_{0,x}) \\ \frac{1}{2}(u_1 + v_{0,x}) & v_1 \end{bmatrix} \ , \ \boldsymbol{\epsilon}_i = \begin{bmatrix} u_{i,x} & \frac{1}{2}(u_{i+1} + v_{i,x}) \\ \frac{1}{2}(u_{i+1} + v_{i,x}) & v_{i+1} \end{bmatrix} \ . \tag{13}$$

It is pointed out that used index i corresponds to the terms multiplied with the power y^i, therefore $\boldsymbol{\epsilon}_i \neq \nabla^s \boldsymbol{u}_i$.

While looking at the decomposed parts it is evident that the first tensor corresponds to the zero order polynomial term, second tensor corresponds to the linear terms, third to quadratic terms, etc. In other words, the strain tensor can be approximated as a sum of finite polynomial strain modes. Consequently, the stress tensor can be written the same way as

$$\boldsymbol{\sigma}_{|\Omega_e} = \boldsymbol{\sigma}_0 + \sum_{k=1}^{n} \frac{y^k}{k!}\boldsymbol{\sigma}_k = \sum_{k=0}^{n} y^k c_k \boldsymbol{\sigma}_k, \qquad \text{where } c_k = (k!)^{-1}. \tag{14}$$

The weakform 9 can be further evaluated as one can take a depth-integral over the terms defined in the coating layer Ω_e. Here, the depth-integral is considered as the integration over the coordinate y in Ω_e. Taking the integral over y in the variational equations gives the following equation (valid only for linear elasticity and uniform layer thickness):

$$\int_\Omega \boldsymbol{\sigma}(\boldsymbol{u}) : \boldsymbol{\epsilon}(\boldsymbol{u}^*)\, \mathrm{d}\Omega + \sum_{i=0}^{n}\sum_{k=0}^{n} \frac{(e)^{i+k+1}}{(i+k+1)i!k!} \int_\Gamma \boldsymbol{\sigma}_k : \boldsymbol{\epsilon}_i \, \mathrm{d}\Gamma = \int_\Gamma \boldsymbol{t} \cdot (\boldsymbol{u}_0^* + \boldsymbol{u}_e^*)\, \mathrm{d}\Gamma \ . \quad (15)$$

From this point, it is clear that all the integrals over Ω_e have become surface integrals over Γ, as also proposed in [19]. Therefore, the two phase problem has become an interface problem, involving only domain Ω and interface Γ, that lies on the domain boundary $\partial\Omega$. Here, the boundary region Γ is located at Γ_0 but represents the previously defined domain Ω_e. Refer to figure 2 for an illustration of the reduced problem. Therefore, the initial problem can be redefined directly on Ω and Γ, where $\hat{y} \in [0, e]$ symbolises now the layer coordinate. The problem can be restated as

$$\boldsymbol{u}_a(x,y) = \begin{cases} \boldsymbol{u}(x,y), & \text{in } \Omega \\ \boldsymbol{u}_0(x) + \sum_{i=1}^{n} P_i(\hat{y})\boldsymbol{u}_i(x), & \text{in } \Gamma \end{cases} \quad (16)$$

with the continuity condition

$$\boldsymbol{u}_0(x) = \boldsymbol{u}(x,0) \ . \quad (17)$$

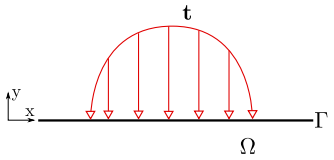

Figure 2: Illustration of the semi-infinite reduced problem around the area of interest.

When looking again at the weakform 15 the interface contribution term in FEM framework can be directly seen as additional interfacial contribution on the underlying element supports in the global stiffness matrix. However, one must also take into account that the resulting local stiffness matrix contribution is a symmetric fully dense matrix. The implementation is similar to finite elements with anisotropic interpolation space (having incomplete polynomial bases) like displayed in [23],[24] or like General Serendipity Elements [25]. These elements have arbitrary shape function orders for different local coordinate directions. Parallels can be made as the proposed approximation coupled to a single element resembles a finite element with higher order approximation in normal direction and linear approximation in tangential direction. However, it must be kept in mind that the resemblance is apparent only regarding the solution space approximation basis. Geometrical representation of the element is different as reduced dimensionality is introduced in the proposed methodology.

The above described method to include thin coating layer contribution on top of existing FE model will be noted from this point forward as Reduced Thin Layer Model, with abbreviation RTLM in short.

2.3. Remarks on simplified cases

It is interesting to note that if the foundation is considered rigid ($\boldsymbol{u} = \boldsymbol{0}$) the equations reduce to an interface contribution

$$\sum_{i=1}^{n}\sum_{k=1}^{n}\frac{(e)^{i+k+1}}{(i+k+1)i!k!}\int_{\Gamma}\boldsymbol{\sigma}_k : \boldsymbol{\epsilon}_i \,\mathrm{d}\Gamma = \int_{\Gamma}\boldsymbol{t}\cdot\boldsymbol{u}_e^* \,\mathrm{d}\Gamma \ . \tag{18}$$

Above equation is representing only the imposed polynomial behaviour of the thin film Ω_e as a surface Γ. One can see this as a generalised version of Matthewson proposed solution [22].

To further simplify the equations, one could take into account only the vertical linear compression mode ($\boldsymbol{u} = 0\boldsymbol{e}_x + \hat{y}v_1\boldsymbol{e}_y$). In this case the following equation is obtained:

$$\int_{\Gamma} C_1 v_1 v_1^* + C_2 v_{1,x} v_{1,x}^* \,\mathrm{d}\Gamma = \int_{\Gamma} p v_1^* \,\mathrm{d}\Gamma, \qquad \forall v_1^* \in \mathcal{U}_0 \ , \tag{19}$$

where the constants are grouped as $C_i = C_i(e, E, \nu)$. From here one can convert the equation to the strong form and see direct correlation with the well known Pasternak foundation model [26], that is widely used in civil engineering. Pasternak model can be presented in reduced dimension as

$$E_k w + G_k w_{,xx} = p \ , \tag{20}$$

where E_k and G_k are parameters connected to the thin film body and the deformed surface is described by the normal displacement of the surface points, $w = v_1 e$.

3. Results

In this chapter the results obtained by the proposed model are presented and analysed. Two different cases will be studied: layer bonded to a rigid substrate and layer bonded to a deformable substrate. Bodies are considered to be semi-infinite like by considering that the dimensions of the domains are large enough for the Dirichlet boundary conditions to not influence the stress distribution near the domain of interest. Refer to figure 3 for illustration. Loading of the domains will be taken according to existing approximations for contact simulations and results are directly compared to analytical results based on corresponding literature. In more complex cases the results are compared to a fully discretized FEM counterpart that will be referred to as the FEM approach.

It is noted that only linear finite elements are considered. One of the expected benefits of RTLM is that it requires no modification to the already existing substrate mesh. Due to mesh conformity requirements this is not the case with higher order isoparametric elements. If higher order isoparametric elements are used for the layer and linear finite

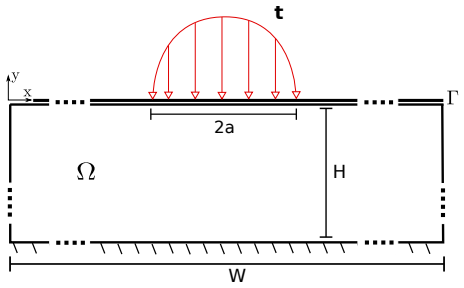

Figure 3: Illustration of the "semi-infinite" domain considered for the numerical analysis. Dimensions of the domain are considered to be large, $a/H = a/W \ll 1$. For illustration purposes the sides are shortened by usage of the symbol "$\cdots$".

elements for the substrate (as often the case in industrial applications) the substrate mesh close to the layer border needs to confirm to the additional nodes of the higher order layer element. Otherwise the discretization will not pass the patch test.

3.1. Layer bonded to a rigid substrate

For the numerical implementation the first consideration is a problem with coating bonded to a rigid substrate. Thus, $\boldsymbol{u} = 0$ in Ω. It allows us to investigate directly the effect of considering polynomial approximation basis for thin layers. One considers very thin coatings defined in the range of $10 \leq a/e \leq 50$.

In the works of Greenwood [5] a semi-analytical solution is provided for a cylindrical indentation of an elastic layer bonded to a rigid substrate. The solution is obtained by the usage of Green function to identify the given indentation shape induced pressure distribution of type

$$p(x) = \sqrt{1-t^2} \sum_{i=0}^{n} d_i t^{2i} \ , \quad \text{where } t = x/a \tag{21}$$

and d_i notes the initially unknown coefficients.

One of the benefits of the Greenwood's approach is to have an unified solution for compressible and incompressible materials. For compressible materials results directly agree with the hypothesis made by Johnson [4] that plane sections of the coating stay plane. Therefore, with RTLM the total penetration is already well captured with order one polynomials. However, if ν is close to 0.5 linear approximation is not sufficient, especially around the contact edges ($x = \pm a$) where significant "pile-up" effect occurs (refer to figure 5). Importance of the effect was first shown by Miller [27]. This is of particular interest as the asymptotic value for the maximum penetration, given by Meijers [2] and Alblas [3] for near incompressible materials can still be approximated with a low order polynomial basis [4]. However, for accurate capture of the "pile-up" effect higher order polynomial approximation is needed, as also noted by Matthewson [22].

In figure 4 the top surface displacement error is presented for the RTLM with different polynomial approximation orders in respect to Greenwood solution[1]. The applied pressure distribution is calculated according to equation 21 with $n = 6$, corresponding to a parabolic indenter shape of $\phi = x^2/2R$, where $R = 50$. The number of nodes in the contact zone for RTLM is fixed to 500.

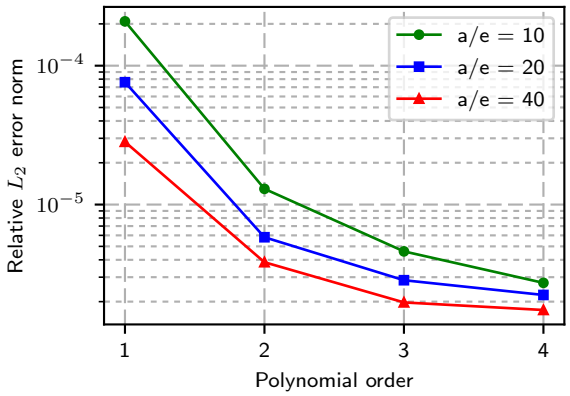

Figure 4: Relative L_2 error norm over $\Gamma(\hat{y} = e)$ for top surface displacement $v(x, y = e)$ according to polynomial order. Used model parameters are $E_c = 0.6$ GPa, $\nu = 0.4$ and ratio of the contact half-width and the layer thickness is noted as a/e.

From the results it is clear that the solution converges with the order of approximation. As the additional gain in accuracy is small for orders above four, there exists no need to consider higher orders. Higher impact on accuracy comes from the underlying foundation element size. For further discussion on this topic refer to section 4.1.

It can be seen that for the considered dimensionless thickness values the results are similar with the exception of having lower error for thinner coatings. This is directly related to the fact that majority of the error is introduced in the edges of the contact where "pile-up" occurs. However, for thinner coatings the "pile-up" influence vanishes as the volume of the pushed material reduces.

To further illustrate the order convergence for the "pile-up" region, refer to figure 5. In sub-figure 5a, the solution is displayed for the case of $\nu = 0.4$ and in 5b for a nearly incompressible material with $\nu = 0.49$. The effect of incompressibility can be clearly seen by the direct difference in the shape and size of the "piles". This also raises the mentioned need for higher orders to capture the correct solution if $\nu \to 0.5$. However, even for the case of $\nu = 0.49$ it seems to be not needed to go higher order than fourth order. The difference between the third and fourth order approximation is small.

[1] Authors point out that in the paper of Greenwood and Barber [5] in Table 2 section b the equation to compute the Green's function includes a misprint error. The term including the residue factors $(A_k \cos(\xi y_k) + B_k \sin(\xi y_k))$ in the definition of $Y(\xi)$ needs to be replaced by $(A_k \sin(\xi y_k) + B_k \cos(\xi y_k))$ as presented in chapter 2 of the same paper.

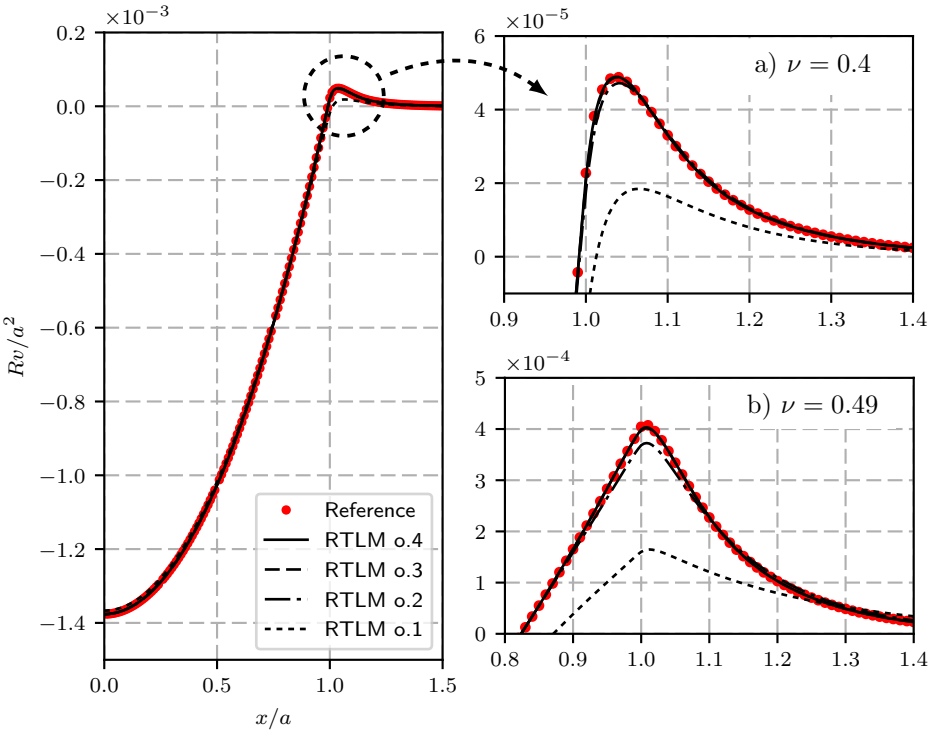

Figure 5: "Pile-up" capture according to polynomial order used. (Results for cases with $a/e = 20$, $R/a^2 = 200$, where shape of indenter is defined as $\phi = x^2/2R$.) Main figure displays the shape of the indentation, whereas a) and b) display close-up views of the "pile-up" region with different Poisson ratio values.

3.2. Layer bonded to a deformable substrate

For the second example the substrate domain Ω is considered elastic. This allows to investigate two cases: same Young moduli $E_c = E_s$ and significantly different moduli $E_c/E_s \ll 1$. If one considers semi-infinite domain the first case corresponds to the Hertzian contact theory and the latter can be directly compared to the FEM approach (with fully discretized layer).

Regarding the $E_c = E_s$ case, the Hertzian pressure distribution is defined as follows [4]:

$$p(x) = \frac{2P}{\pi a^2}(a^2 - x^2)^{1/2} \ , \tag{22}$$

where P denotes the total applied load. In the given example the emulation of the semi-infinity is done as previously explained. The width and height of the square domain is chosen to be large enough to neglect the boundary introduced errors. Illustration can be again seen in figure 3. In figure 6 the interfacial stress between the two subdomains Ω and Γ are shown together with compressive and shear stress along the symmetry axis. Plot illustrates the coupling of the discretized FE domain Ω and the interface Γ with polynomial approximation. The solution corresponds to the Hertz theory.

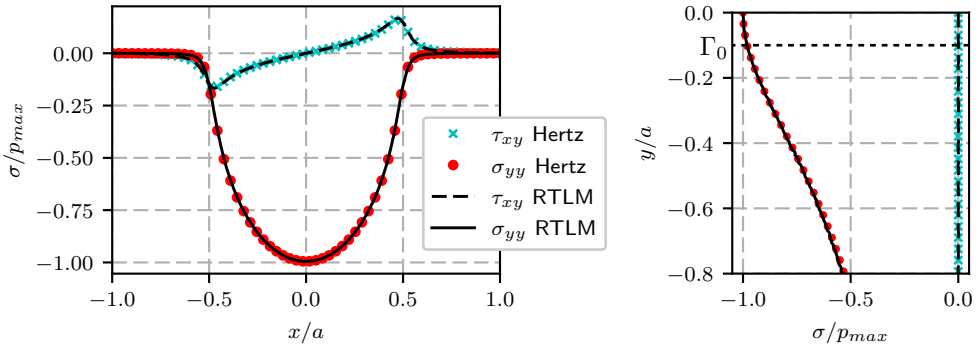

(a) Interface (b) Symmetry axis

Figure 6: Shear and compressive stresses along a) interface $\Gamma(\hat{y} = 0)$ and b) symmetry axis (x=0), with parameters $E_s = E_c = 200$ GPa, $\nu = 0.4$, $p = 3$, $a/e = 10$.

Now, by imposing $E_c/E_s \ll 1$ the Hertz theory is not anymore applicable. Thus the resulting fields can be compared to the fields obtained by more traditional FEM approach. The discretization of the substrate is identical for both simulations. The applied pressure is still defined by the equation 22 and parameters considered are $a/e = 10$, $E_s = 200$ GPa and $\nu_s = 0.3$. However, the coating parameters are taken to represent the expected range of an example of polymer on steel coating system. This type of systems can be found in tubular connections in the OCTG sector. Coating properties are redefined as $E_c = 0.6$ GPa and $\nu_c = 0.45$.

In figure 7 the comparison of the top surface displacement for the RTLM solution with order 3 and FEM approach is presented. The final thickness directional discretization of the layer in the FEM approach is defined according to a mesh convergence study. This lead to 32 elements through the thickness of the coating. The substrate domain meshes are identical for both models. The results provide a good fit.

To further validate the model the reader can refer to chapter 4.1 with figure 8, where p convergence analysis is presented in comparison to the reference FEM test-case.

4. Computational aspect

4.1. Analysis of cost

The main problem in considering thin surface coatings in large scale simulations is the computational cost needed to capture the deformation of the layer. To investigate the cost to accuracy ratio of the proposed method the comparison to the FEM approach counterpart is considered. This is done by considering identical substrate meshes for both cases. Thus, the width of the elements in the interface between the substrate and the layer is fixed. Therefore, accuracy can only be increased by additional refinement of the quadrilateral elements in the normal direction for the FEM approach or by increasing the approximation order for the RTLM case.

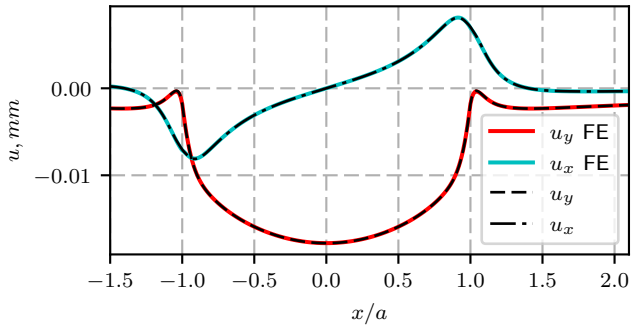

(a) Displacements along $\Gamma(\hat{y} = e)$ (top surface)

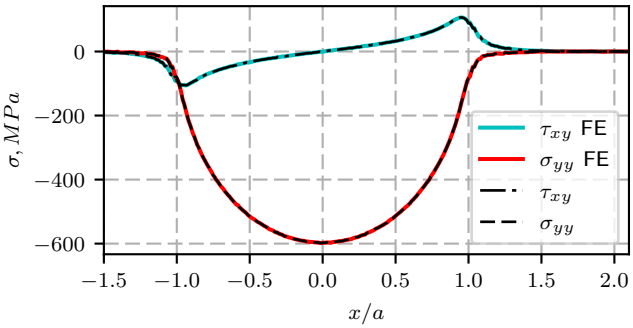

(b) Stress along $\Gamma(\hat{y} = 0)$ (coating substrate interface)

Figure 7: Displacement and stress comparison for RTLM and FEM with applied pressure.

As mentioned before, the figure 8 displays the accuracy to dofs based cost estimation. Analysis is based on the previously explained rigid foundation problem. Pressure distribution is defined according to equation 21, where error is computed in regard to the Greenwood's solution itself. Regarding the cost, RTLM outperforms the considered FEM approach in given simple example by having around three times higher rate of convergence. This gives ground to expect significant reduction of cost for implementing it in more complex models.

On the other hand, often the substrates are discretized without considering the possible coating layer mesh. Therefore, having coarser elements in the substrate mesh near the coated boundary. For investigation of this the same problem as for the deformable substrate case is considered, but with less elements in the contact zone. The results are presented in figure 9. Error is estimated according to highly refined FEM model of the identical problem.

Regarding cost, the RTLM again outperforms the FEM approach. This is mainly due to FEM requirement of additional mesh refinement in the tangential direction to capture the "pile-up" effect on the contact boundaries. Moreover, the RTLM introduces higher order terms in all directions. This allows for improved capture of the "pile-up". However,

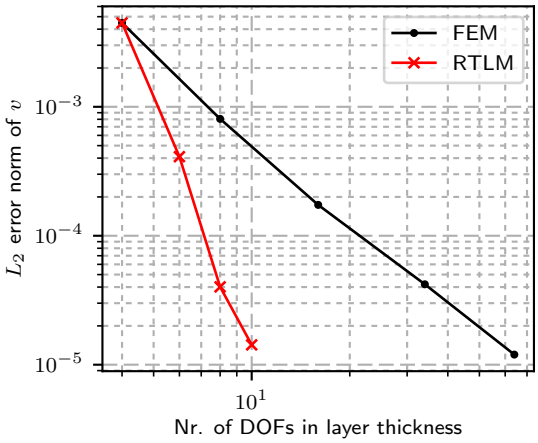

Figure 8: Convergence of the two methods with fixed element widths, based on L_2 error norm of the top surface vertical displacement and the number of dofs stacked on an underlying node position. Simulation with 500 elements underlying the surface layer in the contact halfwidth and $\nu = 0.49$.

the limit still exists as the approximation is still connected to the size of the underlying element through the continuity condition. Therefore, also the proposed method will benefit from additional refinement. Nonetheless, already with order three expansion one has obtained similar accuracy limit as the FEM approach with uni-directional refinement. This accuracy limit is achieved with more than two times less dofs.

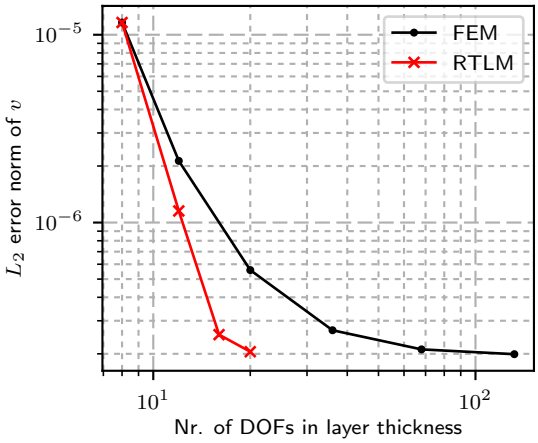

Figure 9: Convergence of the two methods with fixed element widths, based on L_2 error norm of the top surface vertical displacement and the number of dofs stacked on a single underlying node position. Simulation with 160 elements underlying the surface layer in the contact region and $\nu = 0.49$.

4.2. Conditioning

One of the problems hampering to consider iso-parametric flat elongated finite elements is the resulting negative effect on the conditioning of the problem, as there exists significant strain in the tangential direction. For example, one can look at the strain extremum that is localized close to the borderline of the contact area. Therefore, it is important to investigate the conditioning of a stiffness matrix in the proposed framework.

A single block of the layer is considered, with geometrical ratio of $e/L = 0.1$. It is described by a stack of finite elements to mimic FEM approach and by polynomial expansion methodology for the RTLM example. For illustration refer to figure 10. While the accuracy of the problem for the FEM approach can be improved by considering vertical refinement of the stack, the conditioning number will unfortunately also increase. This is due to the increase of the geometrical aspect ratio of a single element. It is also known that by approximating the space with a power series, one also introduces ill-conditioning. The conditioning number is expected to increase exponentially with higher orders [28]. In figure 11 the conditioning numbers of the resulting matrices are compared.

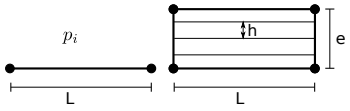

Figure 10: Illustration of the element configurations used in conditioning evaluation. Left is proposed method with series order variable p_i and on right is the finite element stack with element height variable h.

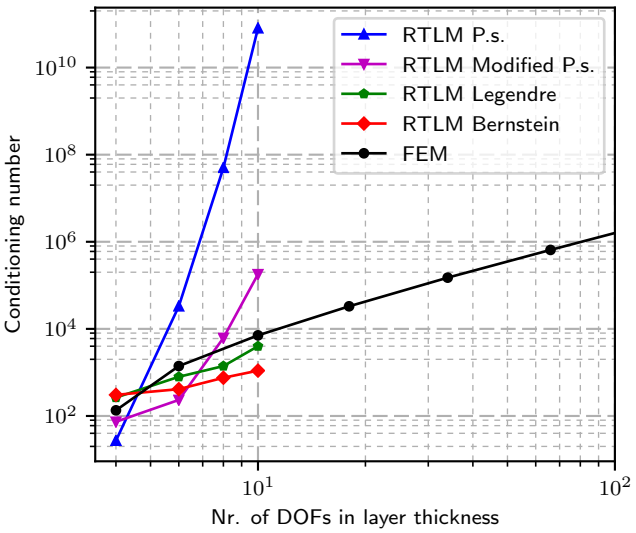

Figure 11: Conditioning number dependency on number of dofs for different polynomial expansion basis.

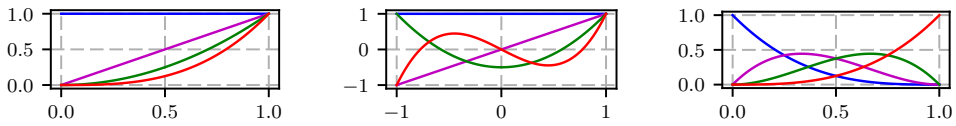

(a) Bounded power series (b) Legendre polynomials (c) Bernstein polynomials

Figure 12: Illustration of different polynomial bases for cubic expansion.

It is clear that considering high order terms is not reasonable as it can introduce high round-off error due to excessive ill-conditioning of the system. However, if one bounds the power series by redefining the series expansion as $P_i(\hat{y}) = \frac{(\hat{y}/e)^i}{i!}$, one can make the conditioning of the stiffness matrix independent from the layer thickness e value. This already brings the conditioning number into reasonable bounds for first four orders of the expansion.

However, the ill-conditioning problem can be completely avoided when introducing polynomial bases with better orthogonality properties, for example Legendre or Bernstein polynomial basis. For illustration of different basis refer to figure 12. One could go even step further and consider polynomial bases with orthogonal derivatives. This would lead to a diagonal stiffness matrix contribution, instead of a full one. However, it is unnecessary as Bernstein, for example, provides low enough impact on matrix conditioning. In addition, it has some interesting properties for inclusion in FEM based contact algorithms, as explained in section 4.3.

4.3. Contact implementation

Previously all the examples have been with applied force that emulates certain contact conditions. This chapter provides a short description on including the proposed methodology in the two body contact problem.

Implementation of the methodology in a FEM contact problem poses one major obstacle. There exists no explicit representation of the contacting surfaces. Therefore, in the closest point projection based contact algorithm, with KKT contact conditions $(t_N \geq 0; g \leq 0; t_N g = 0)$, the gap function $g(\boldsymbol{x} \in \Gamma_e)$ must be modified to take into account the deformable coating layer. Thus the gap function needs to be redefined as $g_e(\boldsymbol{x} \in \Gamma(\hat{y} = e))$ rendering the contact algorithm directly dependent on the polynomial expansion.

However, the direct dependency can be removed by explicitly defining the movement of the contacting surface $\Gamma(\hat{y} = e)$ by additional dofs. In case of the power series the top surface $\Gamma(\hat{y} = e)$ displacement $\boldsymbol{u}_m$ can be simply defined as $\boldsymbol{u}_m = \boldsymbol{u}_0 + e\boldsymbol{u}_1 + \frac{e^2}{2!}\boldsymbol{u}_2 + ... + \frac{e^n}{n!}\boldsymbol{u}_n$. This leads to an unmodified gap function that is defined on the explicitly represented deformable surface: $g(\boldsymbol{x} \in \Gamma(\hat{y} = e))$. In general, the additional displacement dofs describing the movement of surface $\Gamma(\hat{y} = e)$ can be found as

$$\boldsymbol{u}_m(x) = \sum_{i=1}^{n} P_i(e)\boldsymbol{u}_i(x) \ . \tag{23}$$

In case of Bernstein polynomials, this additional set of dofs $\boldsymbol{u}_m$ is not needed, as the beginning and end points of the domain have only single set of non-zero shape function values. Refer to figure 12c. This leads directly to $\boldsymbol{u}_m(x) = \boldsymbol{u}_n(x)$. Therefore, in addition to low conditioning impact, the Bernstein polynomial basis is an interesting candidate to be used in a contact simulation.

4.4. Comment on implementation in general usage FEM codes

From here, it is straightforward to see the potential of implementing the methodology in any FEM contact algorithm. The existing contact enforcement algorithm remains untouched. Only requirement is that the software permits user defined additional stiffness contribution. An example of this has been implemented in ABAQUS 2014 software [29] on a rigid indenter example, as depicted in figure 13. This was done by using the user subroutine UELMAT to define the additional stiffness matrix contribution due to the added surface layer. Bernstein polynomial basis was used for the expansion.

It is necessary to define additional dofs to describe the displacement modes in the layer. However, as ABAQUS has allocated dof structure for the user defined element (UEL), these dofs were introduced via additional nodes on $\Gamma(\hat{y} = e)$. Lagrange and Penalty contact enforcement schemes were used without any modifications. As ABAQUS contact algorithm requires elemental description of the contacting surface "zero-stiffness" membrane elements were defined on the nodes on $\Gamma(\hat{y} = e)$. This was needed to provide an explicit description of the contacting surface for the contact interface tracking.

Figure 13 displays the contact induced pressure distribution obtained by the RTLM implementation in ABAQUS software, for an indentation simulation with indenter of shape $\phi = x^2/2R$. It is shown that the expected analytical solution from Greenwood [5] is obtained for the case of $a/e = 5$.

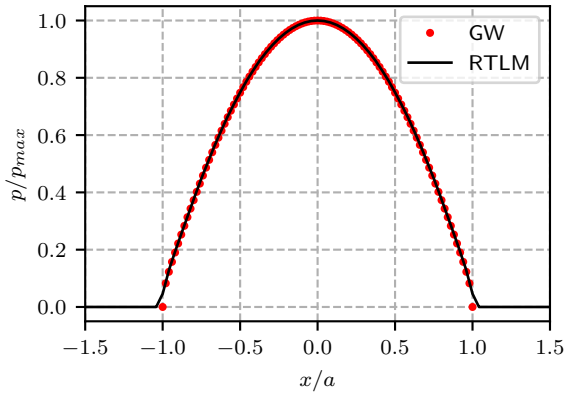

Figure 13: Comparison of the resulting pressure distribution for Greenwood solution (GW) and RTLM contact simulation implemented in ABAQUS. (Indenter of shape $\phi = x^2/2R$, where $R = 50$ and $a/e = 5$.)

5. Conclusion

By considering an alternative approach to model soft thin surface coatings in FEM framework the computational cost linked to traditional approaches could be significantly

reduced.

An efficient numerical model for thin surface layer simulation has been formulated for inclusion in FEM algorithms. The model, named RTLM, involves polynomial expansion based approximation of the solution field, allowing to reduce the volumetric layer representation to an interface contribution. Thus, the additional computational effort to solve the linear system of equations is considerably lower than for traditional FEM approach with fully discretized volumetric layer.

The polynomial based approximation of the layer can be seen as an additional contribution to the global stiffness matrix, making it highly compatible with FEM framework. As matter of fact, it is compatible with any FEM software that allows for user defined stiffness contribution. This includes general contact solvers as no additional modification of the contact algorithm is required. Furthermore, with correct choice of the polynomial approximation basis the effect on the conditioning of the linear system is negligible. Expected ill-conditioning can be avoided by usage of Bernstein polynomial basis, for example. The validity of using polynomial based approximation of the layer is derived from literature and has an excellent agreement with presented 2D test-cases. Higher order polynomials could be used for improved capture of the "pile-up" effect at the boundaries of the contact zone, especially for near incompressible materials.

The proposed idea shows great potential for reducing the cost of considering soft thin coatings in contact simulations. The avoidance of full volumetric discretization and suitability for FEM algorithms makes RTLM a feasible option for consideration in more complex mechanical systems. This includes large scale 3D contact simulations with finite deformations, nonlinear material models and inclusion of wear.

References

[1] V. M. Aleksandrov, Asymptotic solution of the contact problem for a thin elastic layer, Journal of Applied Mathematics and Mechanics 33 (1) (1969) 61–73.

[2] P. Meijers, The contact problem of a rigid cylinder on an elastic layer, Applied Scientific Research 18 (1) (1968) 353–383.

[3] J. Alblas, M. Kuipers, On the two dimensional problem of a cylindrical stamp pressed into a thin elastic layer, Acta Mechanica 9 (3-4) (1970) 292–311.

[4] K. L. Johnson, Contact mechanics, Cambridge university press, 1987.

[5] J. Greenwood, J. Barber, Indentation of an elastic layer by a rigid cylinder, International Journal of Solids and Structures 49 (21) (2012) 2962–2977.

[6] I. Argatov, G. Mishuris, Frictionless elliptical contact of thin viscoelastic layers bonded to rigid substrates, Applied Mathematical Modelling 35 (7) (2011) 3201–3212.

[7] I. Argatov, Contact problem for a thin elastic layer with variable thickness: Application to sensitivity analysis of articular contact mechanics, Applied Mathematical Modelling 37 (18-19) (2013) 8383–8393.

[8] I. Argatov, G. Mishuris, Contact mechanics of articular cartilage layers, Springer, 2015.

[9] I. G. Goryacheva, Contact mechanics in tribology, Vol. 61, Springer Science & Business Media, 2013.

[10] M. B. Rubin, Cosserat theories: shells, rods and points, Vol. 79, Springer Science & Business Media, 2000.

[11] Z. Hashin, Thin interphase/imperfect interface in elasticity with application to coated fiber composites, Journal of the Mechanics and Physics of Solids 50 (12) (2002) 2509–2537.

[12] Y. Benveniste, T. Miloh, Imperfect soft and stiff interfaces in two-dimensional elasticity, Mechanics of materials 33 (6) (2001) 309–323.

[13] Y. Benveniste, O. Berdichevsky, On two models of arbitrarily curved three-dimensional thin interphases in elasticity, International Journal of Solids and Structures 47 (14-15) (2010) 1899–1915.

[14] D. Givoli, Finite element modeling of thin layers, Computer Modeling In Engineering And Sciences 5 (6) (2004) 497–514.
[15] C. Sussmann, D. Givoli, Y. Benveniste, Combined asymptotic finite-element modeling of thin layers for scalar elliptic problems, Computer Methods in Applied Mechanics and Engineering 200 (47-48) (2011) 3255–3269.
[16] J. Yvonnet, H. L. Quang, Q.-C. He, An xfem/level set approach to modelling surface/interface effects and to computing the size-dependent effective properties of nanocomposites, Computational Mechanics 42 (1) (2008) 119–131.
[17] M. Rubin, Y. Benveniste, A cosserat shell model for interphases in elastic media, Journal of the Mechanics and Physics of Solids 52 (5) (2004) 1023–1052.
[18] M. Dragon-Louiset, On a predictive macroscopic contact-sliding wear model based on micromechanical considerations, International Journal of Solids and Structures 38 (9) (2001) 1625–1639.
[19] M. Dragon-Louiset, C. Stolz, Approche thermodynamique des phénoménes liés á l'usure de contact, C. R. Acad. Sci. Paris t. 327, Série II (b) (2000) 1275–1280.
[20] C. Stolz, A thermodynamical approach of contact wear as application of moving discontinuities, Arch. of Appl. Mech. 77 (2007) 165–175.
[21] C. Stolz, A thermodynamical approach of moving interfaces: application to friction and wear, Entropy 12 (6) (2010) 1418–1439.
[22] M. J. Matthewson, Axi-symmetric contact on thin compliant coatings, Journal of the Mechanics and Physics of Solids 29 (2) (1981) 89–113.
[23] O. Zienkiewicz, R. Taylor, The Finite Element Method Vol. 1, Heinemann, 2000.
[24] R. L. Taylor, On completeness of shape functions for finite element analysis, International Journal for Numerical Methods in Engineering 4 (1) (1972) 17–22.
[25] A. Ball, The interpolation function of a general serendipity rectangular element, International Journal for Numerical Methods in Engineering 15 (5) (1980) 773–778.
[26] P. Pasternak, On a new method of an elastic foundation by means of two foundation constants, Gosudarstvennoe Izdatelstvo Literaturi po Stroitelstuve i Arkhitekture (1954).
[27] R. Miller, Some effects of compressibility on the indentation of a thin elastic layer by a smooth rigid cylinder, Applied Scientific Research 16 (1) (1966) 405–424.
[28] G. Strang, G. J. Fix, An analysis of the finite element method, Vol. 212, Prentice-hall Englewood Cliffs, NJ, 1973.
[29] ABAQUS, Dassault Systemes Simulia Corp, Johnston, RI, USA (2014).